Machine Vision and Applications (2010) 21:677–686
DOI 10.1007/s00138-009-0206-y

SPECIAL ISSUE PAPER

Towards automatic power line detection for a UAV surveillance system using pulse coupled neural filter and an improved Hough transform

Zhengrong Li · Yuee Liu · Rodney Walker · Ross Hayward · Jinglan Zhang

Received: 31 August 2008 / Accepted: 22 June 2009 / Published online: 1 September 2009

Abstract Spatial information captured from optical remote sensors on board unmanned aerial vehicles (UAVs) has great potential in automatic surveillance of electrical infrastructure. For an automatic vision-based power line inspection system, detecting power lines from a cluttered background is one of the most important and challenging tasks. In this paper, a novel method is proposed, specifically for power line detection from aerial images. A pulse coupled neural filter is developed to remove background noise and generate an edge map prior to the Hough transform being employed to detect straight lines. An improved Hough transform is used by performing knowledge-based line clustering in Hough space to refine the detection results. The experiment on real image data captured from a UAV platform demonstrates that the proposed approach is effective for automatic power line detection.

Keywords Machine vision · Power line inspection system · Unmanned aerial vehicles (UAVs) · Hough transform · Pulse coupled neural filter · Knowledge-based system

Z. Li (✉) · Y. Liu · R. Hayward · J. Zhang
School of Information Technology,
Queensland University of Technology, Brisbane, Australia
e-mail: zhengrong.li@student.qut.edu.au

R. Walker
Australian Research Center for Aerospace Automation,
Queensland University of Technology, Brisbane, Australia
e-mail: ra.walker@qut.edu.au

Y. Liu
e-mail: yuee.liu@qut.edu.au

R. Hayward
e-mail: r.hayward@qut.edu.au

J. Zhang
e-mail: jinglan.zhang@qut.edu.au

1 Introduction

Surveillance and maintenance of electrical infrastructure is a critical issue for the reliability of electricity transmission. Inspection and management of vegetation around power lines is a significant cost component of maintenance of the electrical infrastructure. For example, Ergon Energy, one of the top electricity companies in Australia, currently spends $80 million a year inspecting and managing vegetation that encroaches on power line assets. Ineffective surveillance could lead to loss of reliability of electricity transmission and produce serious hazards (e.g. the power outages that happened in Canada and USA in 2003) [1,2]. Currently, most electricity companies use calendar-based ground patrols [3]. However, calendar-based inspection by linesman is labor-intensive, time consuming and expensive. It also results in some zones being inspected more frequently than needed and others not often enough.

Satellites and aerial vehicles can pass over more regularly and automatically than the ground patrol. Therefore, remote sensing data captured from satellite and airborne sensors have great potential in assisting power line corridor monitoring. Two critical limitations for using current satellite sensors are the unfavorable revisit time and lack of choice in optimum spatial and spectral resolutions [4]. Airborne platforms are an alternative, but the traditional piloted airborne platforms are limited by their high operational costs. Remote sensors mounted on unmanned aerial vehicles (UAVs) have the potential to fill this gap, by providing a cheap and flexible way to gather spatial data from power line corridors. They can also meet the requirements of spatial, spectral, and temporal resolutions. Overhead power line inspection in remote and rural areas is an ideal application for UAVs because of the lower population density and large distribution of power line network. UAVs can fly relatively close to the power line, providing a cheap and flexible way to gather spatial data in the power line corridors. In order to achieve automatic power line surveillance and inspection using UAVs, power line extraction is required because (1) it is useful for guiding the UAVs flying along the line and automatically collecting data in power line corridors; (2) risk assessment of power lines and the adjacent trees is meaningful only when power lines can be recognized.

There has been very limited investigation involved in developing algorithms for automatic extraction of power lines from aerial images because power lines in traditional aerial images are too small to be detected due to the flight height and resolution of the camera. Although straight line detection is a common and well-studied research area in machine vision, most of the existing algorithms take bottom-up approaches which just use the intensity of single pixels. However, the qualitative performance of these algorithms varies widely across application domains as our notion of what constitutes a line can vary from one application area to another. Due to the wide variation of line types encountered in the UAV images that are not of interest, we require a more top-down approach that takes advantage of our understanding of lines in this application area.

In this research, we combine the bottom-up and top-down approaches and propose a knowledge-based technique specifically for power line detection in aerial images. The proposed method is tested on real image data captured from a UAV platform in Queensland rural areas.

The remainder of the paper is structured as follows. Section 2 briefly introduces related work in power line extraction. In Sect. 3, our proposed approaches are described in detail. Section 4 presents and discusses the experimental results and Sect. 5 concludes our work.

2 Related works

Most of the energy companies use geographic information systems (GIS) to record locations of their assets (e.g. power poles), from which power line information can be inferred. However in general, the accuracy of such information is only suitable as a guide. For an automatic power line inspection system using machine vision, the major problem focuses on how to effectively extract power lines from complicated image backgrounds.

Automatic power line detection from aerial imagery is a rather challenging task, especially when the background is cluttered. There has been very limited investigation involved in developing algorithms for the automatic power line extraction due to the low resolution of traditional aerial images. Some work on the visual control of an UAV for power line inspection has been simulated using a laboratory test rig [5]. They proposed an automatic power line detection method based on Hough transform, but the approach was just a simulation of straight line detection and not evaluated in real image data. More recently, the Radon transform was used to extract line segments of the power lines, followed by a grouping method to link each segment, and a Kalman filter was finally applied to connect the segments into an entire line [6]. Although some properties of power lines in the aerial image were discussed, the algorithms in [6] just focus on straight line detection, image edges and other mistakable linear features which are similar to power lines were not considered.

3 The proposed method

The Hough transform is an effective tool for detecting straight lines in images, thus it is a natural choice for the task of automatic power line detection. In real applications of straight line detection, an edge detector is often used to remove irrelevant data and reduce the computational cost prior to the Hough transform being employed. However, the application of classic edge detectors to the aerial images has demonstrated that they are sensitive to image noise, due to complex and irregular ground coverage. In this paper, we take advantage of the characteristics of power lines in aerial image and propose a filter based on a simplified pulse coupled neural network (PCNN) model. This filter can simultaneously remove the background noise as well as generate edge maps. After this, an improved Hough transform is used by performing knowledge-based line clustering in Hough space to refine the detection results.

3.1 Characteristics of power lines

Based on our observation, power lines in aerial image have the following characteristics:

1. A power line has uniform brightness and the color looks different from upward and downward views. Viewing from the ground, the power line is usually dark, whereas viewing from the sky, the power line is brighter than the background simply because it is made of specific metal and has larger light reflection.
2. A power line approximates a straight line although power line sag often exists. Due to the limited coverage area of a single image, the widths of power lines in the image tend to be similar. In addition, the lengths of power lines in one image are similar and the power line is usually the longest line as it crosses the entire image.
3. Power lines are approximately parallel to each other. Due to the forward angle of the imaging sensor and deviation from center, power lines in the image are not completely parallel. However, the intersection of two power lines

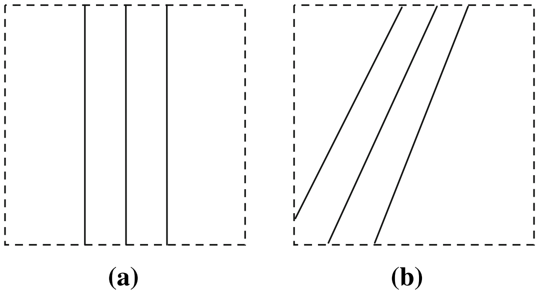

Fig. 1 Power lines from different perspectives: **a** from the above view, **b** from the forward view and offset centre

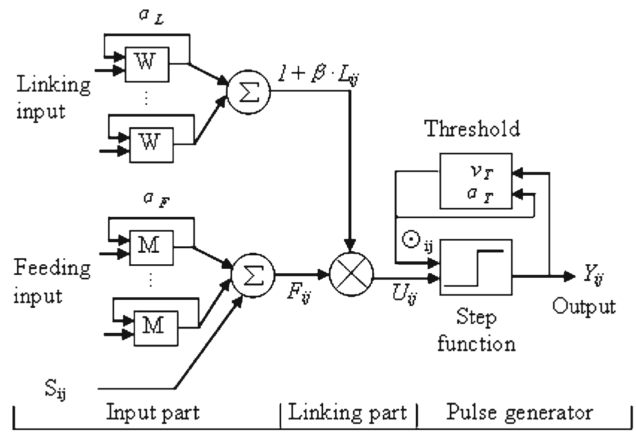

Fig. 2 The structure of PCNN neuron [9]

usually occurs far out of range of the image due to the limited size of images, and the intersecting angle of two lines is usually very small. A simplified illustration is shown in Fig. 1.

3.2 Design of pulse coupled neural filter

Given that power lines are metallic, they have different solar reflectance compared to other background materials (e.g. grass, soil, and bitumen). This knowledge can be used for preliminary detection of power lines from aerial images. Using a filter to remove the irrelevant information will be helpful to reduce the false detection rate as well as the computational cost of line detection algorithm. Threshold filtering may be a practical solution. However, it is not robust because filtering by a threshold is sensitive to image noise and different thresholds may be required due to changing light conditions of the captured images. In this paper, a pulse coupled neural filter (PCNF) is developed for preliminary detection of power lines as well as edge map generation.

The pulse-coupled neural network is a relatively new biologically inspired approach based on the understanding of visual cortical models of small mammals [7]. Unlike other neural networks, the processing is automatic and there is no training involved in PCNN. The time signatures generated from PCNN has the ability to extract edge information, texture information, and to segment the image. This is very useful for image recognition engines.

3.2.1 Standard PCNN model

Most of the PCNNs are based on the Eckhorn model [8]. When applied to image processing a PCNN is a single layered, two-dimensional, laterally connected neural network of pulse coupled neurons. Each neuron corresponds to one pixel in an input image, receiving its corresponding pixel's color information (e.g. intensity) as an external stimulus. The neuron also connects with its neighboring neurons, receiving local stimuli from them. Thus, every neuron can be represented as a specific structure as shown in Fig. 2.

Fig. 3 Linking weight matrix W_L

$1/\sqrt{2}$	1	$1/\sqrt{2}$
1	1	1
$1/\sqrt{2}$	1	$1/\sqrt{2}$

The input part imports external and local inputs to the neuron by the feeding and linking part, respectively. In the linking part, external and local stimuli are combined in an internal activation system, which accumulates the stimuli until it exceeds a dynamic threshold, and then the pulse generator produces a pulse output. Through iterative computation, PCNN neurons produce temporal series of pulse outputs. Similarities in the input pixels cause the associated neurons to pulse synchronously, thus indicating similar structures or textures. These temporal series of pulse outputs contain information of input images and can be utilized for various image processing applications, such as image segmentation, edge detection, feature generation, noise reduction, etc. [10].

This standard PCNN model is usually described by the following five coupled equations:

$$F_{ij}(t) = S_{ij} + \mathrm{e}^{-\alpha_F} \cdot F_{ij}(t-1) + V_F \cdot (M * Y(t-1))_{ij} \tag{1}$$

$$L_{ij}(t) = \mathrm{e}^{-\alpha_F} \cdot L_{ij}(t-1) + V_L \cdot (W * Y(t-1))_{ij} \tag{2}$$

$$U_{ij}(t) = F_{ij}(t) \cdot (1 + \beta \cdot L_{ij}(t)) \tag{3}$$

$$Y_{ij}(t) = \begin{cases} 1 & U_{ij}(t) > \Theta_{ij}(t) \\ 0 & \text{Otherwise} \end{cases} \tag{4}$$

$$\Theta_{ij}(t) = \mathrm{e}^{-\alpha_\Theta} \cdot \Theta_{ij}(t-1) + V_\Theta Y_{ij} \cdot (t-1) \tag{5}$$

where, t is the iteration step, F_{ij} is the feeding input, L_{ij} is the linking input, S_{ij} is the intensity of pixel (i, j), W and M are the weight matrices, * is the convolution operator, Y is the output of neurons; U is the internal activity, β is the linking

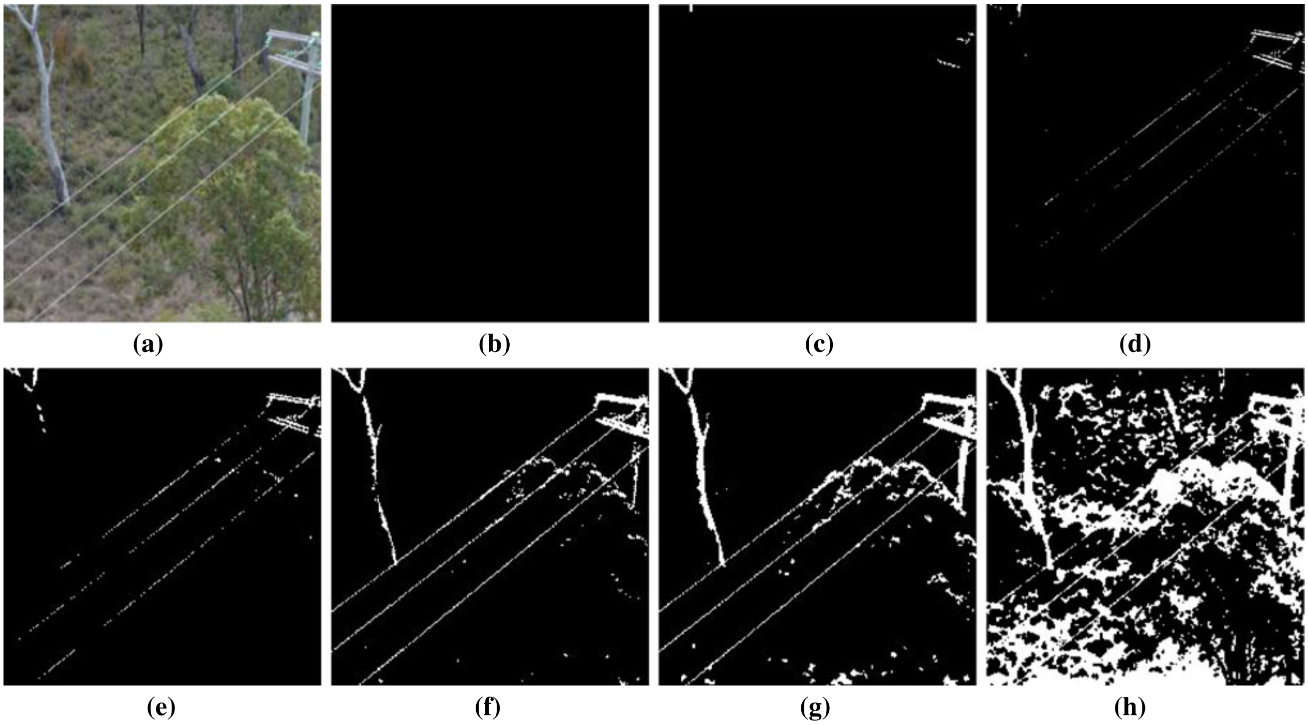

Fig. 4 Original image and seven pulsed outputs of PCNN. **a** Original image, **b** $n = 1$, **c** $n = 2$, **d** $n = 3$, **e** $n = 4$, **f** $n = 5$, **g** $n = 6$, **h** $n = 7$

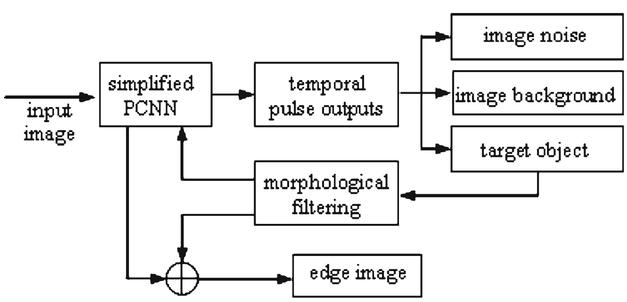

Fig. 5 The structure of pulse coupled neural filter

strength; Θ are the dynamic thresholds; α_F, α_L and α_Θ are the feeding, linking and threshold delay coefficients respectively; V_F, V_L and V_T are the feeding, linking and threshold magnitude scales, respectively. The dynamic thresholds of all neurons are 0 at $t < 1$.

3.2.2 *A filter based on simplified PCNN*

One of key problems of using PCNN is selecting the network parameters. The relationships of network parameters and performance in image analysis is still not clear [7]. There are many parameters in the standard PCNN model that it is hard to select appropriate parameters for various image analysis tasks. In addition, the classic PCNN model involves high computation cost because temporal dependence between iterations is explicitly used in the feeding, linking and threshold updating components. In this paper, a simplified model is developed inheriting the characteristics of classic PCNN model and is described by Equations 6–10:

$$F_{ij}(t) = \text{quantized\_}I \tag{6}$$

$$L_{ij}(t) = \sum_{k,l \in K} W_{Lkl} \times Y_{kl}(t-1) \tag{7}$$

$$U_{ij}(t) = F_{ij}(t) + \beta \times L_{ij}(t) \tag{8}$$

$$Y_{ij}(t) = \begin{cases} 1 & U_{ij}(t) > \Theta_{ij}(t) \\ 0 & \text{other} \end{cases} \tag{9}$$

$$\Theta_{ij}(t) = \begin{cases} \Theta_{ij}(t-1) - \text{step} \\ V_T \times \Theta_{ij}(t) \ \text{ if } Ya_{ij}(t-1) \neq 0 \end{cases} \tag{10}$$

The symbols in Equations (6–10) represent the same meanings as in the standard PCNN model by Equations (1–5).

We simplified the feeding input to be just external stimuli from image data and stimuli from neighboring neurons are not considered. This simplified model still keeps the characteristics of the classic PCNN in that temporal dependence is implicitly included as the neuron outputs in the linking part come from the previous iteration. In this paper, original RGB images are transformed to HIS color space and the intensity component I is used as the feeding input. Moreover, the intensity component is uniformly quantized to 64 levels in order

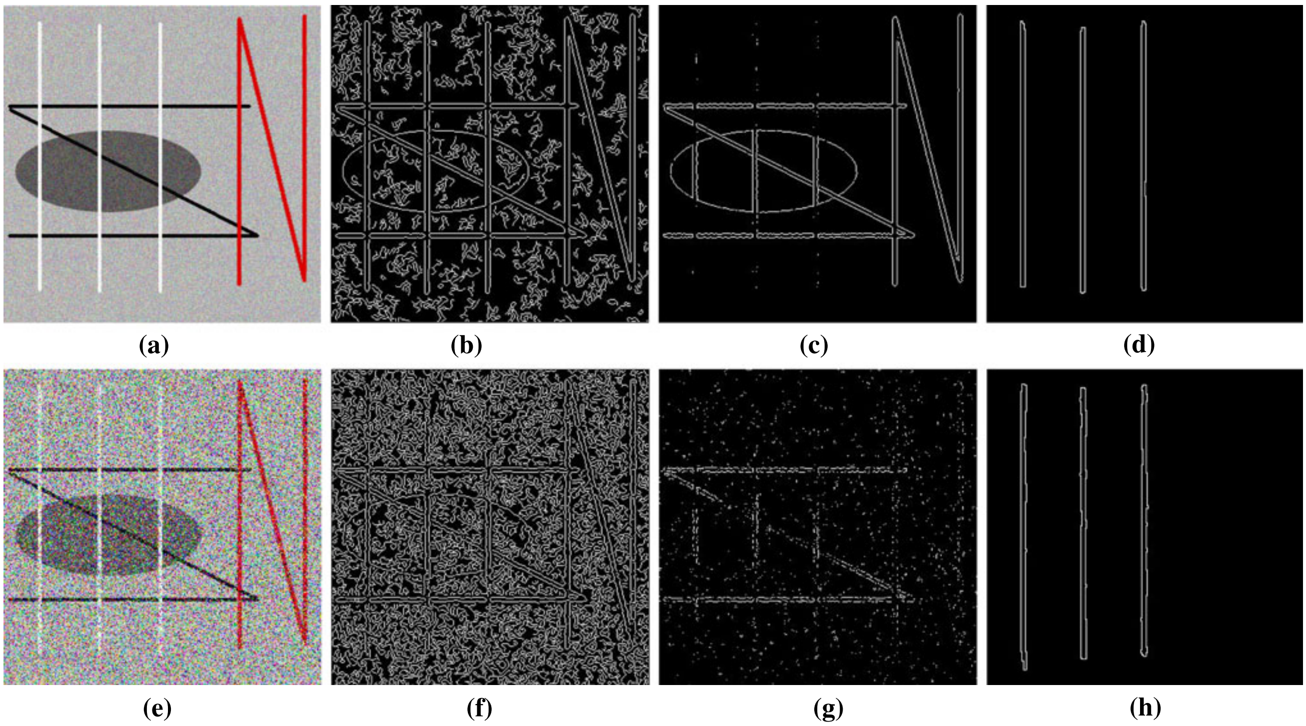

Fig. 6 Comparison of Canny filter, Sobel filter and PCNF. **a** Original image, **b** Canny filter on (**a**), **c** Sobel filter on (**a**), **d** PCNF on (**a**), **e** noised image, **f** Canny filter (**e**), **g** Sobel filter on (**e**), **h** PCNF on (**e**)

to reduce the intensity variation in image regions. This is helpful for filtering regions with similar intensities.

The linking input has also been simplified in that only eight (i.e. 3×3 window) neighbors are adopted in the linking weight matrix W_L. Each element in W_L is the reciprocal of Euclidean distance between this element and the centre of the window (Fig. 3). In this case, neighboring neurons with the closer distance have greater impact on the central neuron. For the calculation of neuron internal status U, a new linear modulation of feeding and linking input is used to avoid zero-valued pixel's influence to the internal status of its neighboring pixels. The linking strength β in this research is set to be 0.2. The pulsed output of neuron Y is binary, and if the neuron pulsed $Y = 1$, otherwise $Y = 0$. Initially Y is set to be a zero-valued matrix. Whether a neuron can pulse or not depends on the comparison of its internal status U with the dynamic threshold Θ. The threshold Θ is initialized to be larger than the maximum value of external stimulus and gradually decays. The dynamic threshold Θ is changing during the iteration operation to control the neuron pulse. If the neuron has been pulsed, a large threshold is given to this neuron by implying a magnitude scale V_T to make sure it will not pulse immediately. Otherwise the threshold of this neuron will be decayed by subtracting a step value.

Given that power lines have higher light reflectance and are usually brighter than the background, they can be roughly detected from the temporal series of PCNN pulsed outputs. In the early stage of the iteration, neurons correspond to power lines pulsed because they have larger external stimulus than most of the background area. Figure 4 shows an aerial image containing power lines and seven temporal pulse outputs in different iterations of PCNN. As is shown in Fig. 4 , in the first iteration of PCNN, no neuron pulses because of the high initial threshold. With the progress of PCNN iteration, neurons corresponding to power lines pulse earlier than other objects in the image. From the temporal outputs of PCNN, different objects of interest can be extracted because PCNN tends to group pixels with similar intensities and structures and also considers spatial relationships among neurons. The temporal information generated by PCNN is also useful for image segmentation and image noise location, which is an advantage over other filters.

In this paper, we use the following rules to locate noisy pixels and remove them based on literature [11]: if pixel (i, j) pulsed and most of its neighboring neurons have not pulsed, then the intensity of this pixel is too large and can be considered as a noisy pixel. Neurons correspond to these noisy pixels pulse earlier than other pixels and thus can be located according to the firing time matrix. For dark noise, the same rule can be applied on the inverse image. Once noisy pixels are located, a median filter is applied to change the intensities of these noisy pixels.

Moreover, edges of the binary pulse outputs can also be detected by using the same PCNN model. The width of the

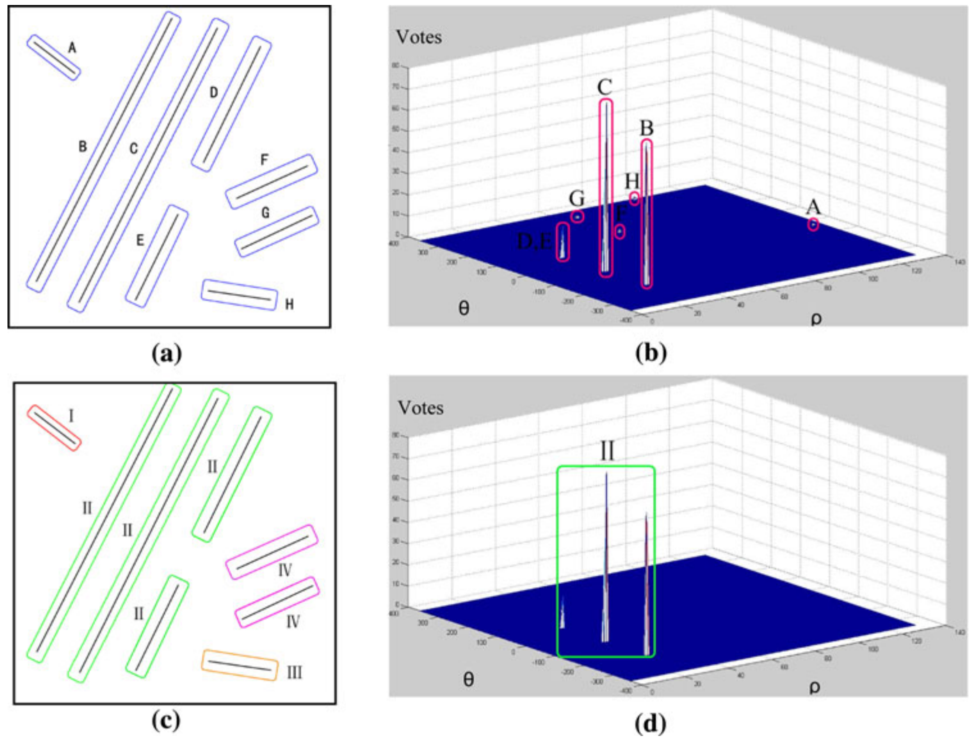

Fig. 7 Voting procedures and the 3D visualization of voting maps. **a** The approximately collinear pixels are clustered into segments A–H. **b** A 3D visualization of the voting map by clustering the approximately colinear pixels. **c** The candidate lines are clustered into four groups (I–IV) according to their angles. **d** The 3D visualization of the voting map by the proposed technique where the group which gain the highest votes are outputed

edge can be determined by controlling the transmitting distance of neuron pulses. In this paper, the following algorithm is used to detect edges in the binary filtered image:

Algorithm 1 Detect edges in binary image using PCNN
Input: binary image Bin
Output: one-pixel width edge set $Edge$

1: initialize the pulse output Y to be the binary image and save it to $Y0$: $Y0 = Y = Bin$
2: calculate the linking input L using equation (7) with 3*3 linking weight matrix
3: calculate the neuron internal status U using equation (8)
4: calculate the output the each neuron using equation (9), with a threshold larger than the minimum value of $U : \Theta = \min(U) + 0.01$; $Y = step(U - \Theta)$
5: the edge of image Bin can be obtained by logical operation exclusive disjunction (XOR) on $Y0$ and Y:

$$Edge = Y0 \oplus Y$$

In summary, our proposed PCNF can be described by Fig. 5. The simplified PCNN is used to generate temporal pulse outputs which contain important information for discriminating image noise, target object (power line) and image background. However, there is no automatic method

Fig. 8 UAV platforms: **a** BAT-3, **b** Eleanor

to determine which output contain power lines and which just contain image noise. According to our experiments, in most cases the output of the third PCNN iteration is a safe choice because pixels corresponding to power lines pulsed and most of the background pixels have not pulsed. After that, morphological filter is applied to the binary pulsed output for post-processing purpose in order to make the detected object more continuous. Finally, the same PCNN model is used to generate the edge image according to algorithm 1.

Figure 6 compares the results using the Canny filter, the Sobel filter and our proposed PCNF on synthetic images with and without noise. The aim of the simulation is try to detect the three light lines in images and generate the edge map. As is shown in figure, Canny and Sobel filters try to detect any edge in the image and are very sensitive to image noises. While the proposed PCNF is more flexible because it can be used to detect the interesting edges rather than all edges in the image. Moreover, PCNF is more robust when the image

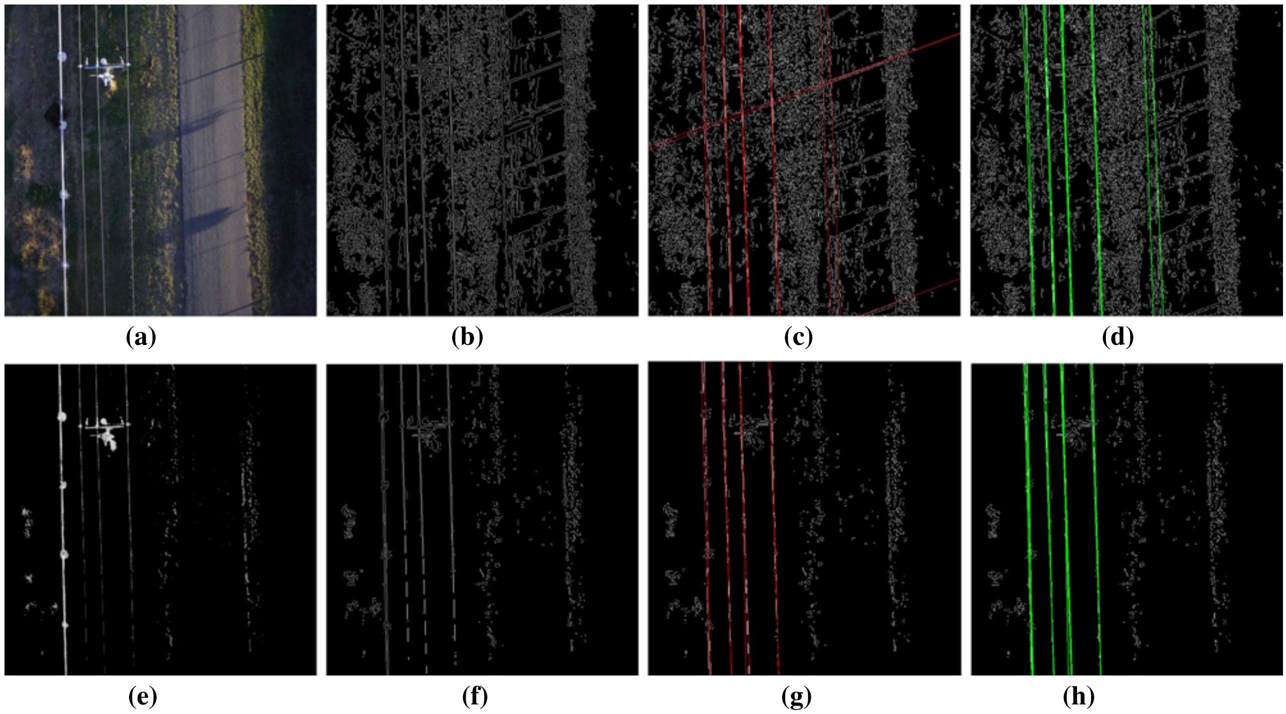

Fig. 9 Comparison of power line detection results. **a** Original image, **b** Canny edge map, **c** Hough line detection on (**b**), **d** knowledge-based post-processing on (**c**), **e** PCNF filtered image, **f** PCNF edge map, **g** Hough line detection on (**e**), **h** knowledge-based post-processing on (**f**)

is contaminated with pepper and salt noise (see the second row of Fig. 6).

3.3 Knowledge-based line clustering in Hough space

Hough transform is used to detect parameterized shapes (e.g. lines, circles) through mapping each point to a new parameter space in which the location and orientation of certain shapes could be identified [12]. When applied to detect straight lines in an image, the Hough transform usually parameterizes a line in the Cartesian coordinate to a point in the Polar coordinate (Fig. 7) based on the point-line duality using the equation:

$$x\cos(\theta) + y\sin(\theta) = \rho \tag{11}$$

Alternatively, this parameterization maps collinear points into a set of intersecting sinusoidal curves in the parameter space. The lines in the Cartesian coordinate can be estimated by detecting points of intersections of these curves (i.e., peaks) in the Polar coordinate [13]. These peaks in the parameter space can be obtained using a voting mechanism.

The Hough transform has proven to be an effective method for line detection. However, it does have some limitations such as high computational cost and mistaken detection of spurious lines. In order to solve these problems, Fernandes and Oliveira proposed an improved Hough transform by introducing a new voting scheme to avoid the brute-force approach of one pixel voting for all potential lines [14]. Instead, the approach operates on clusters of approximately collinear pixels using an oriented elliptical-Gaussian kernel that models the uncertainty associated with the best-fitting line with respect to the corresponding cluster. Figure 7a, b shows their voting procedures and the 3D visualization of voting maps, respectively. The letters A–H indicate the clustered segments that voted to each peaks. In this paper, we extended this improved Hough transform for power line detection purpose.

Hough transform is an effective tool to detect straight lines, but does not intelligently identify power lines. Any linear objects will be detected, such as edge of roads and rivers, fences, etc. Although using PCNF can significantly decrease the influence of other linear edges, problem still exist especially when the linear object has similar color with power lines. In order to discriminate power lines from other linear objects, we use a k-means algorithm to cluster all detected lines to identify the lines of interest.

The objective of data acquisition in our project is to achieve a low flying altitude where a typical 12 mm transmission lines will be represented by at lease two pixels. Therefore, each power line is detected as at least two Hough lines in the edge image. Power lines are almost parallel with very similar angles, and a power line is usually the longest line as it crosses the entire image, while other detected lines do not have this regular property. Based on this idea, a cluster schema is employed in the Hough transform voting procedure to group the parallel lines and output the cluster with largest summation of votes as candidate powerlines (as shown in Algorithm 2). Figure 7c, d illustrates this clustering schema and show the 3D visualization of voting maps. Parallel lines are grouped together and the cluster with largest summation of votes indicates that the dominate lines of the image are in this cluster.

Algorithm 2 Knowledge-based line clustering in the Hough space

Input: detected Hough line set $Ls(\rho, \theta, votes)_i (i = 1, 2, \ldots, n)$, where n is the number of detected lines, ρ and θ are the coordinates of pixels in Hough parameter space, $votes$ is the accumulate number of votes of each detected Hough line.

Output: candidate power lines $CPLs$

1: calculate the line groups $C_j (j = 1, 2, \ldots, k)$ using K-means on θ values of $Ls_i (i = 1, 2, \ldots n)$, where k is the number of line clusters (in this paper we choose $k = 4$).
2: calculate the summation of votes in each cluster $SumVotes_j = \sum_{j=1}^{k} Ls(votes)_i$
3: find the cluster C_m with largest value of *Sum Votes*, where $SumVotes_m = \max(SumVotes_j)$ $(j = 1, 2, \ldots k)$
4: output the lines in cluster C_m as candidate power lines $CPLs = C_m$

4 Experiment and discussion

The experiment is performed on real image data captured from two UAV platforms: V-TOL Aerospace *BAT-3*, and ARCAA UAV platform *Eleanor* (Fig. 8).

In the experiment, we compare Hough line detection results on edge maps generated from Canny and our proposed PCNF. The results before and after using knowledge-based line clustering in Hough space are also compared. As is shown in Fig. 9a, there are many linear features in the original image: power lines, edges of road, shadows, etc. These linear features are detected by Hough transform (see Fig. 9c). Although some of these lines can be eliminated by applying knowledge-based post-processing, lines such as road edges are not removed because they are parallel to power lines (see Fig. 9d). A better choice is trying to avoid the misleading information before detecting power lines. In this paper, we use the proposed PCNF for preliminary detection of power lines and edge map generation. It can be seen from Fig. 9e that most irrelevant points are filtered, though some noise still exists. This is because PCNF has the characteristic of grouping pixels according to the space or gray similarity. It reduces the local gray differences of images and makes up local tiny discontinuous points in image regions. Power lines are made of metal and have uniform brightness on images while the background is different on textures and intensities. Neurons stimulated by power lines generate different spectral stimuli from that of the background, and then they pulse non-synchronously. Thus, power lines are discriminated from the background. According to our experiment, pulse output of PCNF at the third iteration is a safe choice because pixels corresponding to power lines pulsed and most of the background pixels have not pulsed at that time. However, automatic selection of temporal pulse outputs is required in the future work. From Fig. 9g, h, we can see that after using PCNF, power lines are correctly detected no matter using knowledge based post-processing or not. It should be mentioned that this approach is not perfect. A metallic fence line is also detected (see the left line in Fig. 9), because it has very similar characteristics with power lines. In Australia, it is not uncommon that the fence lines are existed in power line corridor and in many cases they are parallel to power lines. Future work is to discriminate these mistaken linear features (e.g. paralleled fence lines) from power lines. Prospective improvement is to discriminate them by incorporating more knowledge. For example, the width of power lines and the spatial relationship with power poles.

Figure 10 shows more results of the experiment. The first row is the original images. Rows 2 and 3 are Hough line detection results on Canny edge image and PCNF edge image without using knowledge-base post-processing. Rows 4 and 5 are the results after using knowledge-based line clustering. From the experiment, it is clear that the proposed PCNF is very useful as a pre-processing tool. Most noise is filtered and the power lines are prominent in the images. After using PCNF, fewer irrelevant lines exist. Applying knowledge-based post-processing by clustering lines in the Hough space also increases the accuracy of power line detection. Combination of these techniques can significantly increase the accuracy of power line detection in the complex environment.

5 Conclusion

In this paper, a novel method is proposed specifically for power line detection from aerial images. First, a PCNF is developed to remove the background noise and generate an edge map prior to Hough transform being employed to detect straight lines. After that, a knowledge-based line clustering is performed in Hough space to refine the detection results. The experiment on real image data captured from our UAV platforms demonstrates that the proposed approach can significantly increase the accuracy of power line detection in complex environments.

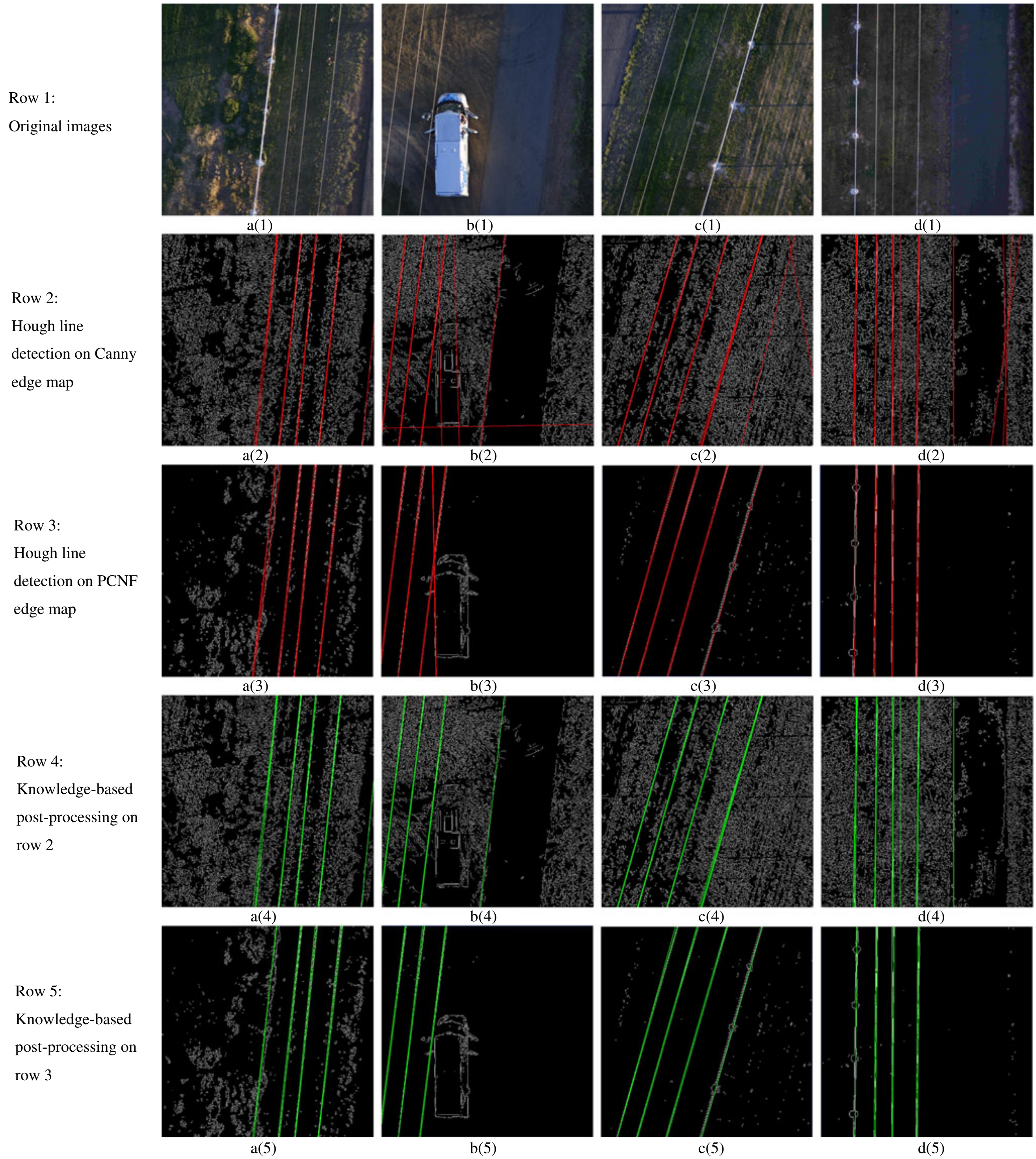

Fig. 10 Experimental results on real image data captured from UAV Platforms

Acknowledgments This work was conducted within the CRC for Spatial Information, established and supported under the Australian Government's Cooperative Research Centers Programme, and in conjunction with the Australian Research Centre for Aerospace Automation (ARCAA).

References

1. Appelt, P.J., Goodfellow, J.W.: Research on how trees cause interruptions- applications to vegetation management. In: IEEE Rural Electric Power Conference. Scottsdale, Arizona (2004)

2. Beck, K., Mathieu, R.: Can power companies use space patrols to monitor transmission corridors? In: ESRI User Group Conference, San Diego (2004)
3. Russell, B.D.: Reliability based vegetation management through intelligent system monitoring. In: Power Systems Engineering Research Center. Texas A&M University, Texas (2007)
4. Berni, J.A.J. et al.: Thermal and narrowband multispectral remote sensing for vegetation monitoring from an unmanned aerial vehicle. IEEE Trans. Geosci. Remote Sens. **47**(3), 722–738 (2009)
5. Golightly, I., Jones, D.: Visual control of an unmanned aerial vehicle for power line inspection. In: 12th International Conference on Advanced Robotics. Seattle, WA (2005)
6. Yan, G. et al.: Automatic extraction of power lines from aerial images. IEEE Geosci. Remote Sens. Lett. **4**(3), 387–391 (2007)
7. Ma, Y. et al.: Principle and Applications of Pulse-Coupled Neural Networks. Science Press, Beijing (2005)
8. Eckhorn, R. et al.: A neural network for feature linking via synchronous activity: results from cat visual cortex and from simulations. In: Cotterill, R.M.J. (ed.) Models of Brain Function, pp. 255–272. Cambridge University Press, Cambridge (1989)
9. Forgáč, R., Mokriš, I.: Formal representation of images by pulse coupled neural networks. In: 3rd Slovakian–Hungarian Joint Symposium on Applied Machine Intelligence. Slovakia (2005)
10. Lindblad, T., Kinser, J.M.: Image Processing Using Pulse-Coupled Neural Networks, 2nd edn, p. 161. Springer, Berlin (2005)
11. Zhang, J., Dong J., Shi, M.: An adaptive method for image filtering with pulse-coupled neural networks. In: IEEE International Conference on Image Processing (ICIP). Genova, Italy (2005)
12. Aggarwal, N., Karl, W.C.: Line detection in images through regularized Hough transform. IEEE Trans. Image Process. **15**(3), 582–591 (2006)
13. Agganval, N., Karl, W.C.: Line detection in images through regularized hough transform. In: International Conference on Image Processing, Vancouver, BC (2000)
14. Fernandes, L.A.F., Oliveira, M.M.: Real-time line detection through an improved Hough transform voting scheme. Pattern Recognit. **41**, 299–314 (2008)